

Sorption of ethene and ethane on the $V_2O_5(001)/TiO_2(001)$ anatase interface

D.C. Sayle, C.R.A. Catlow

Royal Institution of Great Britain, 21 Albemarle Street, London W1X 4BS, UK

M.A. Perrin and P. Nortier

Centre de Recherche de Rhône-Poulenc, 52 Rue de la Haie Coq, 93308 Aubervilliers, France

Received 21 August 1995; accepted 11 January 1996

Simulation techniques have been employed to investigate the differences in the low energy adsorption configurations of ethene and ethane on the TiO_2 supported and unsupported $V_2O_5(001)$ surface. We find that the ethene molecule approaches much closer to the *supported* $V_2O_5(001)$ surface which is reflected in the 40 kJ mol^{-1} higher adsorption energy. The low energy adsorption configuration located for ethane on the supported V_2O_5 shows that the molecule does not approach as close to the supported V_2O_5 surface as does ethene, resulting in the adsorption energy of ethane being 52 kJ mol^{-1} lower than that of ethene on the supported V_2O_5 surface.

Keywords: selective oxidation; V_2O_5 catalysts; computation; simulation

1. Introduction

Thin V_2O_5 (monolayer) films supported on TiO_2 (anatase) may exhibit catalytic properties (for example the selective oxidation of hydrocarbons) which cannot be attributed to either the unsupported V_2O_5 surface or the TiO_2 substrate [1–9]. The activity and selectivity of such supported catalysts is directly related to the surface sites of the supported thin film [10–12]. A study of these sites will lead to a better understanding of the catalysis effected by these materials and may aid the design of supported catalysts with improved activity and selectivity for particular chemical reactions.

In a previous study [13], we showed, using atomistic computer simulation methods, that the structure of the anatase supported V_2O_5 monolayer is significantly modified from that of the unsupported V_2O_5 . This present study extends these earlier calculations by investigating the adsorption of ethene and ethane on the surface of the supported V_2O_5 thin films. The low energy configurations and sorption energies are then compared with the sorption of such molecules on the unsupported V_2O_5 . Differences in the sorption behaviour of the molecule almost certainly influence the catalysis. The low energy adsorption sites identified can also be employed as starting configurations for more computationally intensive quantum mechanical calculations which will be used in future studies of the reaction mechanisms involved in the partial oxidation reactions promoted by the catalyst.

2. Simulation methods and potential models

As in our previous study [13], we use the standard surface simulation procedure available in the MARVIN program [14] to model the unsupported and supported monolayers onto which, in the present study, both ethene and ethane are adsorbed. The crystal is considered as a stack of planes periodic in two dimensions. The stack is divided into two regions; a region I, where the ions are allowed to relax explicitly and a region II, where the ions are held fixed relative to each other. Region II is included to ensure that the long range effects of the ions in the bulk of the crystal on the surface region are correctly represented. In normal surface simulations the top of region I is the free surface and an interface is created if two dissimilar materials are placed together.

The interionic potentials for the oxides were based on the Born model of the ionic solid, which includes a long range Coulombic interaction and a short range term to model the Pauli repulsions and van der Waals attractions between the component ions. The shell model [15] describes the electronic polarisability of the component ions. Potential parameters for V_2O_5 are taken from Dietrich, Catlow and Maigret [16] and for TiO_2 , from Sayle et al. [13]. Intramolecular potentials for ethene and ethane were taken from the BIOSYM cvff.frc molecular mechanics forcefield [17]. Intermolecular potentials between the molecule and V_2O_5 or TiO_2 were taken from Vetrivel, Catlow and Colbourn [18]. The potential parameters are all listed in table 1(a–f).

Table 1

Potential parameters employed in this study: O and O1 correspond to the vanadyl oxygen and bridging oxygen of V_2O_5 respectively and O3, the oxygen of TiO_2 . H and C are hydrogen and carbon of ethene, H3 and C3, hydrogen and carbon of ethane. (a) Two-body terms of the Buckingham analytical form: $V(r) = A \exp(-r/\rho) - Cr^{-6}$. (b) Two-body terms of the Lennard-Jones analytical form: $V(r) = Ar^{-12} - Br^{-6}$. (c) Two-body terms of the Morse analytical form: $V(r) = D_e \{1 - \exp[-\lambda(r - r_0)]\}^2$. (d) Three-body terms of the analytical form: $V(r) = 0.5K[\Theta - \Theta_0]^2$. (e) Four-body terms of the analytical form: $V(r) = K[1 + S \cos(\text{Phase} - \Phi)]$. (f) Shell model parameters, the analytical function of the core-shell energy is of the form: $V(r) = 0.5Kr^2$, where r is the core-shell separation

(a)	Species	A (eV)	ρ (Å)	C (eV Å ⁶)			
	V-O	2549.73	0.341	0.0			
	V-O1	5312.99	0.268	0.0			
	V-O2	5312.99	0.268	0.0			
	O-O	22764.3	0.149	23.0			
	O-O1	22764.3	0.149	23.0			
	O-O2	22764.3	0.149	23.0			
	O1-O1	22764.3	0.149	23.0			
	O1-O2	22764.3	0.149	23.0			
	O2-O2	22764.3	0.149	23.0			
	Ti-O	175000.0	0.171	0.0			
	Ti-O1	175000.0	0.171	0.0			
	Ti-O2	175000.0	0.171	0.0			
(b)	Species	A (eV Å ¹²)	B (eV Å ⁶)				
	O-H	1557.522	5.574				
	O1-H	1557.522	5.574				
	O2-H	1557.522	5.574				
	O-H3	1557.522	5.574				
	O1-H3	1557.522	5.574				
	O2-H3	1557.522	5.574				
	O-C	15118.161	22.579				
	O1-C	15118.161	22.579				
	O2-C	15118.161	22.579				
	O-C3	11825.615	17.661				
	O1-C3	11825.615	17.661				
	O2-C3	11825.615	17.661				
(c)	Species	D_e (eV)	λ (Å ⁻¹)	r_0 (Å)	Cutoff (Å)		
	V-O	10.0	2.302	1.58	5.0		
	C-H	3.920	2.000	1.09	1.4		
	C-C	7.103	2.000	1.33	1.6		
	C3-H3	4.709	1.771	1.10	molecular mechanics ^a		
	C3-C3	3.816	1.915	1.53	molecular mechanics ^a		
(d)	Species	K (eV)	Θ_0 (deg.)	Cutoff (Å)			
	O2-Ti-Ti	57.793	99.23	2.1	2.1	3.2	
	C-C-H	1.466	121.2	1.60	1.30	2.9	
	C3-H3-H3	1.713	106.4	molecular mechanics			
	C3-H3-C3	1.925	110.0	molecular mechanics			
(e)	Species	K (eV)	S	Phase			Cutoff (Å)
	H-C-C-H	0.707	-1	2	1.3 1.6 1.3		
	H3-C3-C3-H3	0.062	1	3	molecular mechanics		
(f)	Species	Charge (e)	K (eV Å ⁻²)				
	O shell	-2.717	54.952				
	O1 shell	-2.717	54.952				
	O2 shell	-2.717	54.952				
	V core	5.0	rigid ion				
	Ti core	4.0	rigid ion				
	C core	-0.290	rigid ion				
	H core	0.145	rigid ion				
	C3 core	-0.021	rigid ion				
	H3 core	0.007	rigid ion				

^a In molecular mechanics, potential interactions are for specified bonds.

The electrostatic potential field surrounding a molecule has been shown to be an important indicator of the way a molecule interacts with its environment [19] and may substantially contribute to sorption energies on polar materials, such as oxides. It is therefore essential to describe these electrostatic interactions accurately. The charges were derived from the electrostatic potential field surrounding the molecules, calculated from ab initio wavefunctions at the Hartree–Fock level with a 6-31G** basis set using the CHELPG approach [20] as implemented in GAUSSIAN92 [21]. The resulting charges on the ethane atoms (reported in table 1f) are much lower than those assigned to the ethene, which is reasonable considering the ethene carbon atoms are sp^2 hybridised compared with the sp^3 carbon atoms of ethane. The higher charges therefore reflect the higher electronegativity of the sp^2 carbon of ethene. The “directional” π -electrons of the ethene are expected to play a significant role in the adsorption of the ethene on the V_2O_5 surface or supported film and should be suitably accommodated within the potential model. Such directional bonding characteristics are not, however, introduced into the present potential model explicitly (for example via three-body terms) as these would be difficult to derive and, furthermore, would be dependent on the surface material on which the ethene is adsorbed. Some of the effects of the π -electrons may be reflected by the higher charges assigned to the sp^2 carbons and may also be implicit within the shape of the ethene molecule.

The surface configurations of the unsupported V_2O_5 and TiO_2 supported V_2O_5 monolayer structures were determined in previous studies [13] where we observed significant structural modifications of the V_2O_5 thin films which have also been observed experimentally [22,23]. To calculate the low energy adsorption configurations of ethene and ethane, the molecule is placed both on the unsupported V_2O_5 surface or the supported V_2O_5 monolayer film and the system relaxed until zero forces act between the component species. To ensure that the lowest energy configurations have been identified, several starting configurations of the molecule are investigated. We note that the adsorption energy is defined as the energy required to remove the molecule from the lowest energy configuration on the surface or interface to a position at infinity.

3. Results and discussion

Our calculations located stable minima for both ethene and ethane adsorbed on the unsupported $V_2O_5(001)$ surface and on the $TiO_2(001)$ anatase supported surface of the $V_2O_5(001)$ monolayer thin film.

3.1. Ethene adsorption

Figs. 1a and 1b show the low energy configuration

for ethene adsorbed on respectively the supported and unsupported $V_2O_5(001)$ surfaces. The ethene molecule adopts a high symmetry configuration when adsorbed on the unsupported V_2O_5 surface. The vanadyl O–O bond distance (4.15 Å) allows the molecule to fit within the $V_2O_5(001)$ surface trough with each of the four hydrogen atoms close to a vanadyl oxygen (fig. 1a). In contrast, the considerable structural modification of the V_2O_5 monolayer, as a result of the anatase support, reduces the high symmetry of the $V_2O_5(001)$ surface and consequently a significant change in the adsorption configuration of ethene is observed (fig. 1b).

On examining the detailed structures of the lowest energy configurations of the sorbed ethene we observe that the molecule is significantly closer to the surface of the supported compared with the unsupported $V_2O_5(001)$ (table 2). For example the H–O (vanadyl oxygen) distance is 0.30 Å shorter and the H–O (bridging oxygen) is 0.85 Å shorter for ethene on the supported surface which is reflected in the 40 kJ mol^{−1} higher adsorption energy (table 3). Clearly the ethene is more tightly bound to the supported V_2O_5 surface. Table 3 also gives the component terms (i.e. short range and Coulombic) of the adsorption energy. It is interesting to note that there is no significant distortion of the surface by the sorbed molecule, in contrast with the studies of molecular clusters at ionic surfaces, which found large perturbations from the perfect relaxed surface [24–26]. The latter, however, relate to dipolar sorbates in contrast to the present case where we are investigating neutral species with zero dipole moments.

3.2. Ethane adsorption

The low energy configurations for sorbed ethane on the unsupported and supported $V_2O_5(001)$ surfaces are shown in figs. 2a and 2b respectively. Table 4 gives the H–O distances for the ethane on the supported and unsupported V_2O_5 . The higher H–O distances (compared with ethene) suggest that the ethane molecule is unable to approach as near to the surface as ethene, which is reflected in the adsorption energy being 52 kJ mol^{−1} lower than for ethene on the supported V_2O_5 .

4. Conclusion

The application of atomistic simulation to the sorption of ethene and ethane on supported V_2O_5 has enabled us to identify low energy adsorption sites for these molecules. We find in particular that the large structural modification of the V_2O_5 , as a direct result of the TiO_2 support, leads to a substantial change in the low energy adsorption configuration for ethene. Indeed, the ethene is more strongly bound to the supported V_2O_5 monolayer by 40 kJ mol^{−1}; such differences are almost

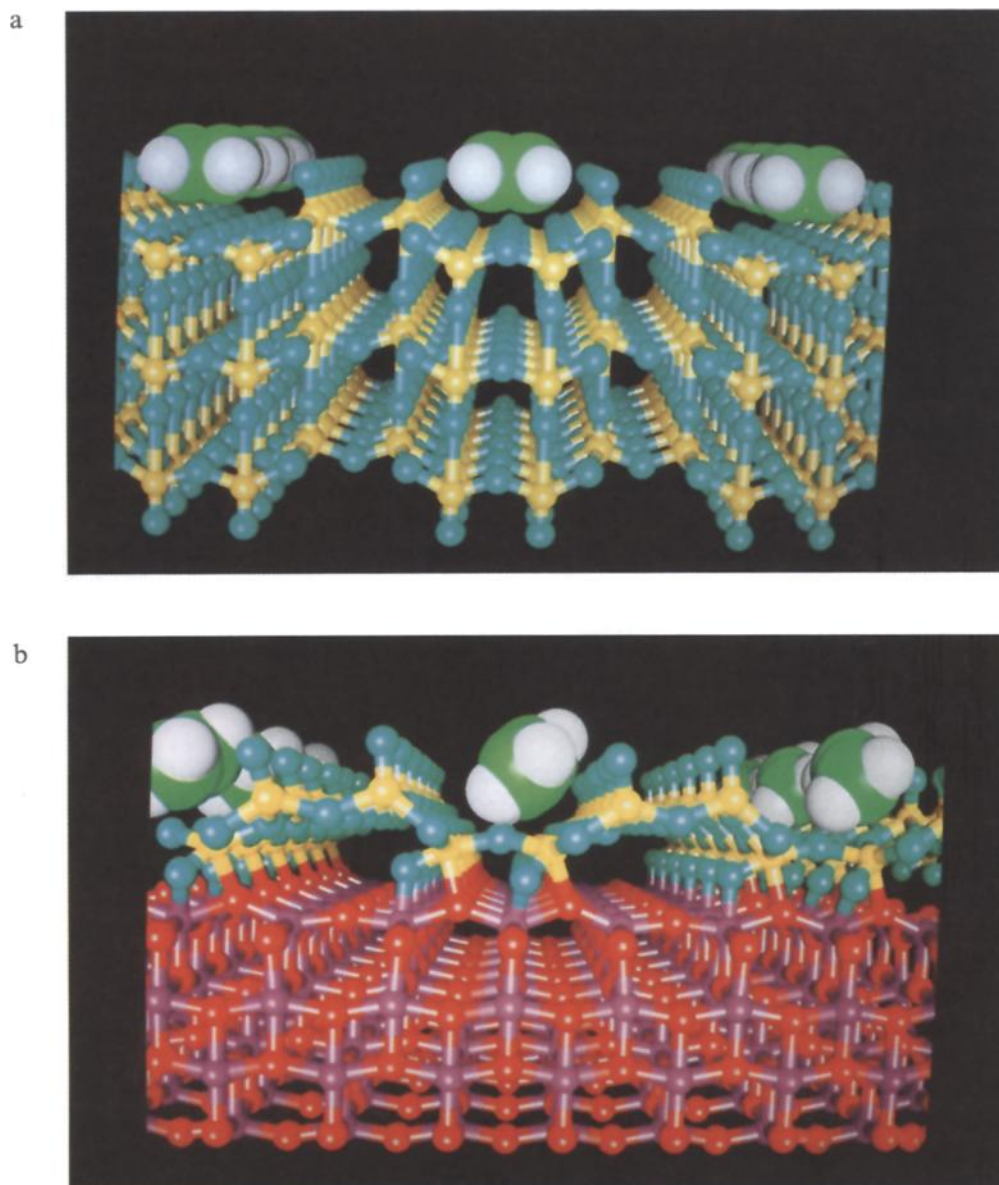


Fig. 1. (a) Ethene adsorbed on the unsupported $V_2O_5(001)$ surface; vanadium is yellow, oxygen (V_2O_5) is green, carbon is light green and hydrogen white. (b) Ethene adsorbed on the monolayer $V_2O_5(001)/TiO_2(001)$ anatase thin film. Titanium is coloured purple, oxygen (TiO_2) is red, vanadium is yellow, oxygen (V_2O_5) is green, carbon is light green and hydrogen white.

Table 2

Bond lengths for ethene on the unsupported $V_2O_5(001)$ surface and monolayer $V_2O_5(001)/TiO_2(001)$ anatase thin film

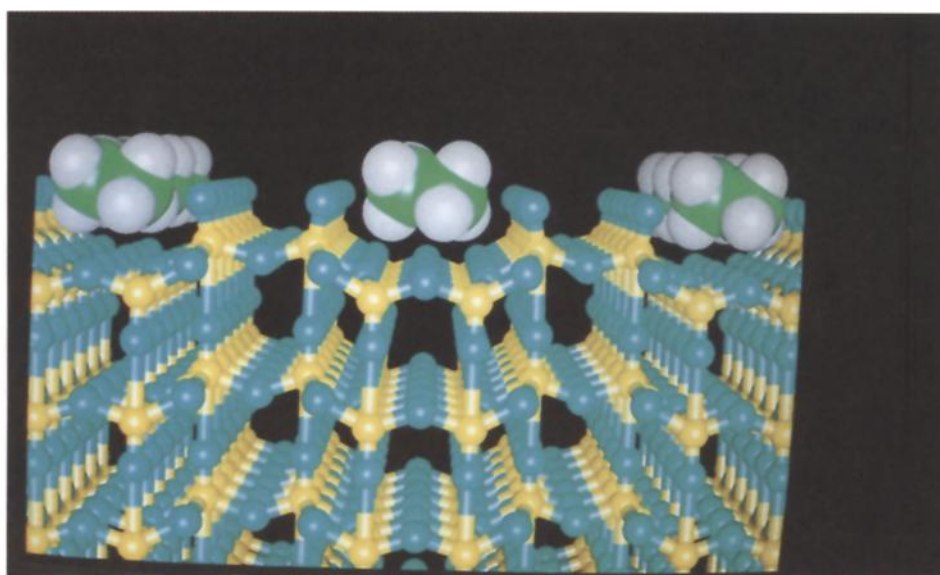
H–O bond lengths (Å)				
C_2H_4 on surface			C_2H_4 on interface	
	vanadyl oxygen	bridging oxygen	vanadyl oxygen	bridging oxygen
H1	2.60	–	2.28	–
H2	2.58	–	–	2.37, 2.74
H3	2.60	–	2.44	2.65
H4	2.58	–	–	2.34, 2.43, 2.43, 2.87, 2.78
C1	–	–	2.99	2.82, 2.99
C2	–	–	–	2.76, 2.86

Table 3

Short range component and Coulombic component terms of the adsorption energies of ethene and ethane adsorbed on the unsupported $V_2O_5(001)$ surface and monolayer $V_2O_5(001)/TiO_2(001)$ anatase thin film

Energy (kJ mol ⁻¹)	C ₂ H ₆ on surface	C ₂ H ₆ on interface	C ₂ H ₄ on surface	C ₂ H ₄ on interface
short range	24.9 (98%)	26.6 (97%)	21.5 (54.2%)	9.6 (12.1%)
Coulomb	0.5 (2%)	0.8 (3%)	18.2 (45.8%)	70.0 (87.9%)
total energy	25.4	27.4	39.7	79.6

a



b

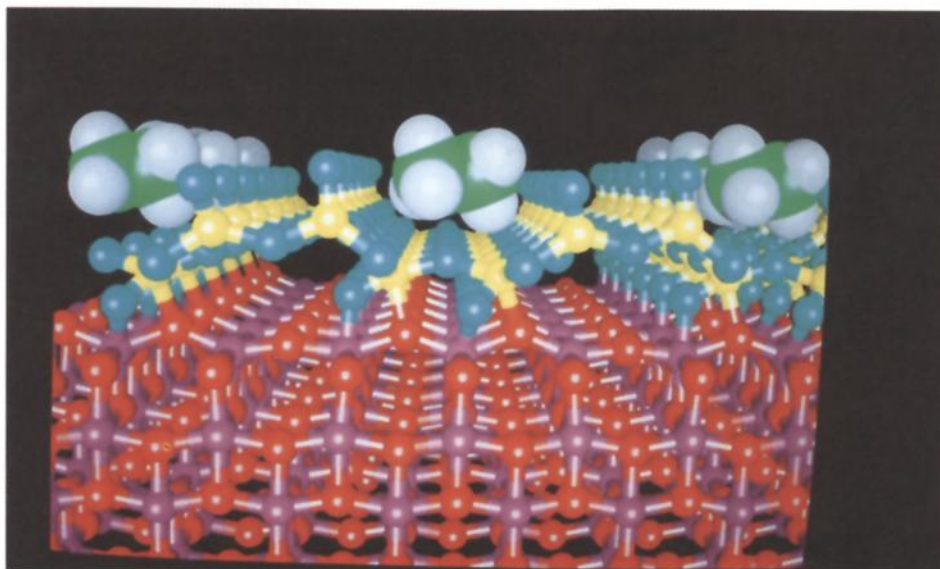


Fig. 2. (a) Ethane adsorbed on the unsupported $V_2O_5(001)$ surface. Vanadium is yellow, oxygen (V_2O_5) is green, carbon is light green and hydrogen white. (b) Ethane adsorbed on the monolayer $V_2O_5(001)/TiO_2(001)$ anatase thin film. Titanium is coloured purple, oxygen (TiO_2) is red, vanadium is yellow, oxygen (V_2O_5) is green, carbon is light green and hydrogen white.

Table 4

Bond lengths for ethane on the unsupported $V_2O_5(001)$ surface and monolayer $V_2O_5(001)/TiO_2(001)$ anatase thin film

	H–O bond lengths (Å)			
	C ₂ H ₆ on surface		C ₂ H ₆ on interface	
	vanadyl oxygen	bridging oxygen	vanadyl oxygen	bridging oxygen
H1	2.87	2.57, 2.79, 2.81	–	2.58, 2.68, 2.72
H2	2.73	–	–	2.72, 2.77
H3	–	–	–	–
H4	–	2.74, 2.86	2.91	2.59, 2.62, 2.70
H5	2.95	2.59, 2.86, 2.93	2.66	–
H6	2.90	–	2.83	–

certainly of relevance to the catalytic processes in this system. Moreover, the identification of such low energy configurations can be employed for more intensive quantum mechanical calculations which may elucidate the reaction mechanisms and pathways for partial oxidative catalysis.

Acknowledgement

We would like to thank Rhône-Poulenc for funding this project and also BIOSYM Technologies for the provision of the INSIGHTII graphical software.

References

- [1] I.E. Wachs, G. Deo, M.A. Vuurman, H. Hu, D.S. Kim and J.M. Jehng, *J. Mol. Catal.* 82 (1993) 443.
- [2] G. Centi, S. Perathoner and F. Trifirò, *Res. Chem. Intermediates* 15 (1991) 49.
- [3] G. Centi, E. Giamello, D. Pinelli and F. Trifirò, *J. Catal.* 130 (1991) 220.
- [4] F. Hatayama, T. Ohno, T. Maruoka, T. Ono and H. Miyata, *J. Chem. Soc. Faraday. Trans.* 87 (1991) 2629.
- [5] T. Machej, M. Remy, P. Ruiz and B. Delmon, *J. Chem. Soc. Faraday Trans.* 86 (1990) 715.
- [6] T. Machej, M. Remy, P. Ruiz and B. Delmon, *J. Chem. Soc. Faraday Trans.* 86 (1990) 723.
- [7] T. Machej, M. Remy, P. Ruiz and B. Delmon, *J. Chem. Soc. Faraday Trans.* 86 (1990) 731.
- [8] G.C. Bond, S. Flamerz and R. Shukri, *Faraday Discussions Chem. Soc.* 87 (1989) 65.
- [9] Z.X. Liu, Q.X. Bao and N.J. Wu, *J. Catal.* 113 (1988) 45.
- [10] A. Satsuma, A. Furuta, T. Hattori and Y. Murakami, *J. Phys. Chem.* 95 (1991) 3248.
- [11] M. Witko, R. Tokarz and J. Haber, *J. Mol. Catal.* 66 (1991) 205.
- [12] S.R.G. Carrazan, P.J. Benitez and V. Rives, *Vibrational Spectroscopy* 5 (1993) 295.
- [13] D.C. Sayle, C.R.A. Catlow, M.-A. Perrin and P. Nortier, *J. Phys. Chem.*, in press.
- [14] D.H. Gay and A.L. Rohl, *J. Chem. Soc. Faraday Trans.* 91 (1995) 925.
- [15] B.G. Dick and A.W. Overhauser, *Phys. Rev.* 112 (1958) 90.
- [16] A. Dietrich, C.R.A. Catlow and B. Maigret, *Mol. Simul.* 11 (1993) 251.
- [17] Biosym Technologies, 9685 Scranton Road, San Diego, USA.
- [18] R. Vetrivel, C.R.A. Catlow and E.A. Colbourn, *J. Chem. Soc. Faraday Trans.* 85 (1989) 497.
- [19] E. Scrocco and J. Tomasi, *Adv. Quantum Chem.* 11 (1978) 115.
- [20] C.M. Breneman and K.B. Wiberg, *J. Comput. Chem.* 11 (1990) 361.
- [21] M.J. Frisch, G.W. Trucks, M. Head-Gordon, P.M.W. Gill, M.W. Wong, J.B. Foresman, B.G. Johnson, H.B. Schlegel, M.A. Robb, E.S. Replogle, R. Gomperts, J.L. Andres, K. Raghavachari, J.S. Binkley, C. Gonzales, R.L. Martin, D.J. Fox, D.J. Defrees, J. Baker, J.J.P. Stewart and J.A. Pople, *GAUSSIAN92*, Revision D.2 (Gaussian, Pittsburg PA, 1992).
- [22] R. Kozłowski, R.F. Pettifer and J.M. Thomas, *J. Phys. Chem.* 87 (1983) 5176.
- [23] J.C. Vedrine, *Catal. Today* 20 (1994).
- [24] D.C. Sayle, PhD Thesis, University of Bath, UK (1992).
- [25] D.C. Sayle, S.C. Parker and J.H. Harding, *J. Mater. Chem.* 4 (1994) 1883.
- [26] A.R. George and K.D.M. Harris, in preparation.